TJES
ISSN: 1813-162X
Tikrit Journal of Engineering Sciences
available online at: http://www.tj-es.com

Experimental Analysis of Heat Transfer Enhancement and Flow with Cu,TiO_2 Ethylene glycol Distilled Water Nanofluid in Spiral Coil Heat

Khalid Faisal Sultan *
Electromechanical Engineering Department, University of Technology, Baghdad, Iraq
E-mail: ksultan61@yahoo.com

(Received 1 June 2014, Accepted 22 February 2017, Available online 30 September 2017)

Abstract

This experimental investigation was performed to improve heat transfer in the heat exchanger (tube of shell and helically coiled) using nanoparticles for turbulent parallel flow and counter flow of distilled water (Dw) and ethylene glycol (EG) fluids. Six types of nanofluids have been used namely: copper – distilled water, copper – distilled water and ethylene glycol, copper – ethylene glycol, titanium oxide – distilled water, titanium oxide – distilled water and ethylene glycol, titanium oxide – ethylene glycol with 0.5%,1%,2%,3% and 5% volume concentration as well as the range of Reynolds number are 4000 – 15000. The experimental results revel that an increase in coefficient of heat transfer of 50.2 % to Cu – Dw, 41.5% to Cu – (EG + Dw), 32.12 % for Cu – EG , 36.5% for TiO_2 – Dw, 30.2 % to TiO_2 – (EG + Dw) and 25.5%, to TiO_2 – EG . The strong nanoconvection currents and good mixing caused by the presence of Cu and TiO2 nanoparticles. The metal nanofluids give more improvement than oxide nanofluids. The shear stress of nanofluids increases with concentration of nanoparticles in case parallel and counter flow. The effect of flow direction insignificant on coefficient of overall heat transfer and the nanofluids behaves as the Newtonian fluid for 0.5%,1%,2%,3% and 5%. Good assent between the practical data and analytical prediction to nanofluids friction factor which means the nanofluid endure pump power no penalty. This study reveal that the thermal performance from nanofluid Cu – Dw is higher than Cu – (EG + Dw) and Cu – EG due to higher thermal conductivity for the copper and distilled water compared with ethylene glycol.

Keywords: Nanofluid, ethylene glycol, enhancement, metallic, nano metallic.

التحليل العملي في تحسينِ انتقال الحرارةِ والجريان للموائع النانوية باستخدام النحاس، وأوكسيد التيتانيوم مع اثيلين كلايكول وماء مقطر في مبادل حراري حلزوني

الخلاصة

تحقيق عملي لتحسين انتقال الحرارة والجريان بواسطة استعمال جزئيات نانوية مثل النحاس وأوكسيد التيتانيوم من خلال مبادل حراري حلزوني مع ماء مقطر واثلين كلايكول وللجريان مضطرب متوازي ومتعاكس. ستّة أنواع مِنْ الموائع النانوية استعملت وهي نحاس- ماء مقطّرَ، نحاس – ماء مقطّرَ وأثيلين كلايكول ، نحاس – إثيلينِ كلايكولَ ، أوكسيد التيتانيوم – ماء مقطّرَ، أوكسيد التيتانيوم – ماء مقطّرَ وأثيلين كلايكول، أوكسيد التيتانيوم - إثيلين كلايكول مع تراكيز حجميه هي 0.5% , 1%, 2%, 3%, 5%. بينت النتائج العملية ان الزيادة بمعامل انتقال الحرارة كانت كالتالي

50.2 % Cu – Dw, 41.5% Cu – (EG + Dw), 32.12 % Cu – EG ,
36.5% TiO_2 – Dw , 30.2 % TiO_2 – (EG + Dw), 25.5%, TiO_2 – EG.

وجود الجزئيات النانوية مثل النحاس واوكسيد التيتانيوم يساهم بتوليد تيارات حمل نانوية قوية وخلط جيد الموائع النانوية التي تحتوي جزئيات نانوية معدنية تكون أكثر تحسين في انتقال الحرارة من الجزئيات النانوية التي تحتوي على اكاسيد نانوية. اجهاد القص للموائع النانوية يزداد مع زيادة التركيز الحجمي للجزئيات النانوية ولجريان متوازي ومتعاكس. ولا

* *Corresponding author: E-mail* : ksultan61@yahoo.com

تأثير لتغير اتجاه الجريان على معامل انتقال الحرارة الكلي وتكون هذه الموائع النانوية هي موائع نيوتنية للتراكيز المأخوذة في الدراسة. وهذه المقالة بينت ايضا ان هناك توافق جيد بين النتائج التجريبيةِ والتحليلية لمعامل الاحتكاك للموائع النانوية. كما واوضحت هذه الدراسة ان الموائع النانوية لأتسبب جزأ بطاقة الضخ. ان الدراسة بينت ان الاداء الحراري للنحاس مع الماء المقطر يكون أفضل من النحاس مع الماء المقطر واثيلين كلايكول وكذلك من النحاس مع اثيلين كلايكول بسبب الموصلية العالية للنحاس والماء المقطر مقارنة مع اثيلين كلايكول.

***الكلمات الدالة*:** مائع نانوي، إثيلين كلايكول، تحسين انتقال الحرارة، نانوية معدني، نانوية غير معدني.

Nomenclature

b	Coil pitch
D	Shell diameter, (m)
d	Diameter of the spiral coiled, (m)
De	Dean number
DW	Distilled Water
E	Roughness of the test tube
EG	Ethylene glycol
f	Friction factor
f_c	Friction factor of coil
k_n	Thermal conductivity of nanofluid, (W/m K)
Pr	Prandl number
R^2	Coefficient of determination
RC	Curvature radius of the coil
Re	Reynolds number
U_0	Overall heat transfer coefficient, (W/m^2 K)

Greek symbols

ΔP	Pressure drop, (Pa)
μ_n	Dynamic viscosity nanofluid, (N s/m^2)
ρ_n	Density of nanofluid, (kg/m^3)
γ	Shear rate, (1/s)
ϕ	Nanoparticle volume fraction

Subscripts

b	Base fluid
c	Counter flow
i	Inlet
n	Nanofluid
p	Parallel flow

Introduction

Heat exchanger are used in various of applications e.g. heating of thermal oil, generation of steam, plants of thermal processing, processing of food and dairy air conditioning, refrigeration and processes of heat recovery. The advantageous cause of helical coil tubes was high coefficient of heat transfer and small size compared with straight tubes. the cost and efficiency of heat exchangers consider very important factors in industry process, there must be exact equation to determine the heat transfer. All engineering applications include heat transfer through a fluid medium such as refrigeration, automobiles, power plants and heat exchangers. Heat transfer in fluids is essentially through convection. However, heat transfer coefficients depend on thermal conductivity of the fluid. To improve the thermal conductivity of a fluid, suspension of solid particles and in general solids thermal conductivity is greater than that of fluids. But the sized nanoparticle include on the mill and micro are liable to plug and deposition in micro channels. on the other hand, nanofluid is stable suspension at a low concentration of nanoparticles. The improvement of fluid thermal conductivity due to dispersed in fluid of the conventional heat transfer without the problems such as plug and deposition. sedimentation and clogging problems. Pak and Cho [1], investigated experimentally the turbulent friction and heat transfer behaviors of dispersed fluids (Al_2O_3 and TiO_2 particles suspended in water) in a circular pipe. Lee et al. [2], observed enhancement of thermal conductivity of nanofluids using CuO and Al_2O_3 nanoparticles with water and ethylene glycol compared to base fluids. The thermal conductivities of nanofluids with CuO and Al_2O_3 nanoparticles have been determined experimentally using steady – state parallel – plate technique by Wang et al. [3], for different base fluids such as water, ethylene glycol and engine oil. The thermal conductivity of these nanofluids increased with increasing volume fraction of the nanoparticles.

Xuan and Li [4], studied the augmentation of thermal conductivity of Cu–water nanofluid for different volume fractions of Cu nanoparticles. Xuan and Roetzel [5], concluded from their findings that the heat transfer enhancement is due to increase in thermal conductivity or due to thermal dispersion caused by random motion of the particles coupled with enhanced thermal conductivity.

Das et al. [6], investigated the variation of thermal conductivity of nanofluids (Al_2O_3 – water and CuO–water) with temperature using temperature oscillation technique. They observed an increase in thermal conductivity with temperature. Yang et al. [7], measured experimentally the convective heat transfer coefficients of several nanoparticles – in – liquid dispersions under laminar flow in a horizontal tube heat exchanger. Koo and Kleinstreuer [8], showed that the Brownian motion has more impact on the thermal properties of nanofluid than thermo – phoresis. Herish et al. [9], have conducted experiment to determine the thermal conductivity of Al_2O_3 – water nanofluid during forced convection in laminar flow through a circular tube with constant wall temperature. Recently Zhang et al. [10], measured the thermal conductivity and thermal diffusivity of Au – toluene, Al_2O_3 – water, TiO_2 – water, CuO water and carbon nanotubes – water nanofluids using the transient short – hot – wire technique. Heat transfers for laminar and turbulent flows in coiled tubes were calculated by Seban and McLaughlin [11]. Regers and Mayhew [12] has been calculated pressure drop and Heat transfer heated helically coiled tubes by using steam heated.

This study indicate that did not get wall temperature of uniform due region was the large core which work the flow of remaining. The objectives of this analysis is to stud characteristics of heat transfer and fluid flow in spiral tube heat exchanger for both parallel flow and counter flow configurations using base fluid and nanoparticles. The effects of nanoparticles concentration and different based fluids such as ethylene glycol, distilled water and ethylene glycol distilled water are investigated.

Nanofluid Preparation

The two – step method was used to prepare nanofluids from base fluid and copper (Cu) or titanium oxide (TiO_2) nanoparticles. Nanoparticles dispersion in three types of base fluid namely: distilled water, ethylene glycol and the mixture of ethylene glycol and distilled water with volume ratio of 60:40. After preparation the nanofluids were put in blending of ultrasonic to half hour due to disperse any nanoparticle aggregation.. The acidic pH is much less than the isoelectric point of these particles, thus ensuring positive surface charges on the particles. The surface enhanced repulsion between the particles, which resulted in uniform dispersions through the experiments. An image nanofluids containing Cu (50nm) and TiO_2 (50nm) are display in Fig. (1).

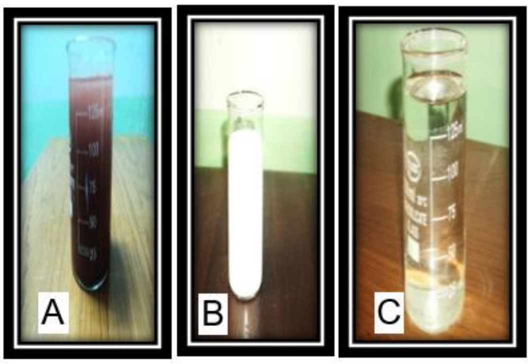

A: Copper–Ethylene glycol
B: Titanium oxide – Ethylene glycol
C: Ethylene glycol

Fig.1. Nanofluids for two types and ethylene glycol.

Analysis of Geometric Shape for Heat Exchanger

Figure (2) reveals geometric shape for heat exchanger (type spiral coiled and shell heat exchange).

The curvature ratio of coil as follows

$$\delta = \frac{d}{2\pi Rc}$$

The non – dimensional pitch as follows

$$\gamma = \frac{b}{2\pi Rc}$$

Dimensionless factors for heat exchanger in this study as follows.

$$Re_i = \frac{\rho V_i d_i}{\mu} \quad , \quad Nu_i = \frac{h_i d_i}{k}$$

$$De = Re_i \left(\frac{d_i}{2Rc}\right)^{0.5} \quad , \quad He = \frac{De}{(1+\gamma^2)^{0.5}}$$

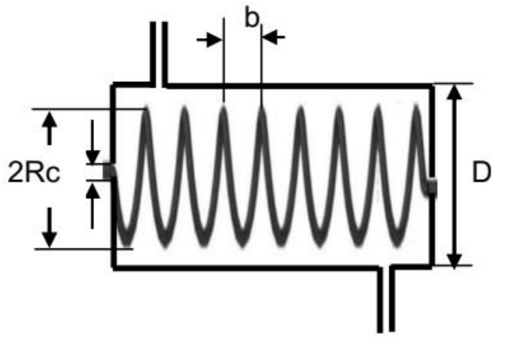

Fig. 2. Geometric shape of heat exchanger.

Mori and Nakayama [13], Experimental investigated on a curved pipe with UHF within large De. These article indicate the two region of the flow firstly BL near the wall while the second to steam condensate on the surface of coil.

Shell – side Reynolds number (Re_o) and Nusselt number (Nu_o) are defined as follow:

$$Re_o = \frac{\rho V_o D_h}{\mu} \quad , \quad Nu_o = \frac{h_o D_h}{k}$$

where: V_o, h_o and D_h are average velocity, convective heat transfer coefficient and hydraulic diameter of shell side respectively.

Experimental Facility and Procedure

The experimental apparatus and schematic diagram used in this work are shown in Figs. (3) and (4) and test section as shown in Fig. (5). The heat exchanger is made of Pyrex (soft glass) and test section is made helically coiled tube of di =10 mm and do=12 mm. Helical tube in this study has 34turns and length of coil is 750 mm. The Pyrex (soft glass) shell has 70 mm inner, 80mm outer diameters and 1000 mm length. The set – up has helically coiled tube side loop and anther side of shell loop. Six types of nanofluids flow in helically coiled tube and this types used copper – distilled water, copper – distilled water and ethylene glycol, copper – ethylene glycol, titanium oxide – distilled water, titanium oxide – distilled water and ethylene glycol, titanium oxide – ethylene glycol. Shell side loop handles hot water.

Fig .3. The Experimental system of the convective heat transfers and flow characteristics for nanofluid.

The studied volume fractions of nanofluids are (Φ = 0.5%,1%,2%,3% and 5%). Shell side loop consist of storage vessel of 20 l capacity with heater of 3.25kW, control valve, water pump and thermostat for temperature. The test section consists of heat exchanger (type shell and spiral tube), pump, needle valve, flow meter within of (0.01–3.5) lpm, cooling unit and storage vessel of 10 liter capacity. Hot water temperature in storage vessel (shell side) is maintained via thermostat. The inlet and outlet temperatures of shell and tube measured by Four T – type thermocouples of 0.15 ^{0}C accuracy.

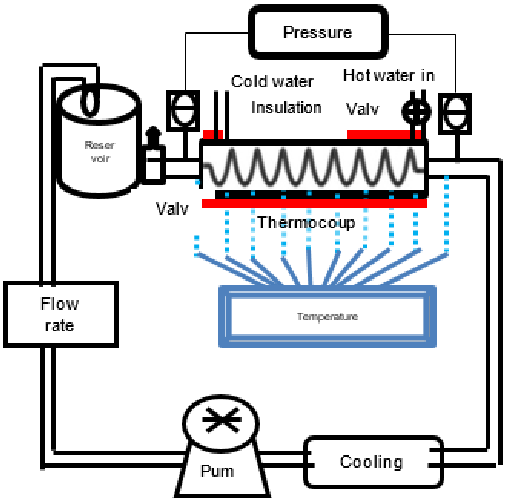

Fig . 4. Schematic diagram of apparatus.

Fig .5. Test section Pyrex spiral annulus.

The wall temperatures of coiled tube were measured by Eight T– type thermocouple. The pressure drop was measured by the pressure gauges are put via the helical tube. The shell is insulated with Acrylic resin coated fiberglass sleeving to minimize the heat loss from shell to the ambient. Distilled water was tested prior to nanofluid after completion of construction and calibration of the flow loop, testing of the loop's functionality for measuring Nusselt number and viscous pressure loss. The numbers of the total tests were 200. At the beginning of experiments was used hot and cold water to check the apparatus from any leakages as well as the thermocouples and thermostat were checked. The six types of nanofluids used in the experiments (Cu – DW,Cu – EG,CU – (EG +DW), TiO_2 – DW, TiO_2 – EG and TiO_2 – (EG+DW)) at 0.5, 1, 2, 3, 5 vol %. The nanofluids with different concentrations will spins during coil tube while pump in shell side will be switched on where Dw will reaching to required temperature. Furthermore, thermostat attached in Dw storage system for this process.

The parallel flow condition was used as the flow configuration at first case. at the steady state were temperatures recorded. This procedure was applied on all concentrations. On the other hand, the counter flow was used in second case, when the flow configuration was changed the same steps used in the counter flow. The volume flow rate in shell was 2.25lpm while the volume flow rate in coil tube was varied. the volume flow rate in coil tube within of (0.75-2) lpm. The range of Reynolds number is (4000–15000).

Measurement of Thermal Properties Nanofluid

The dynamic viscosity (μ) is measured using brook field digital viscometer model DV–E. Figs. (6) and (7) show the comparison between the practical measurement of dynamic viscosity with the empirical relation of Einstain, 1956 model [14], Brinkman, 1952 model [15], Wang et al. model [16] and Batchel model [17]. Figures (8) and (9) represent viscosity for the two types of nanoparticles Cu and TiO_2 with three types of the base fluids DW, EG, EG+DW. The following equipment's was used to measured thermal properties (ρ,μ,K,Cp) respectively. Density executed by weighing a sample and volume, viscometer model (DV – E), Hot Disk thermal constants analyzer (6.1) and specific heat apparatus (ESD – 201), Moreover the measurements of experimental for the density indicated that good agreement with the calculated values from theory of mixing [18] as shown in Figs. (10) and (11). The Figs. (12) and (13) reveal density for the six types of nanofluids. Figures (14) and (15) indicated the experimental measurements to thermal conductivity was compared with thermal conductivity models for many researchers such as Wasp model [19], Hamilton and Crosser [20], Maxwell model [21] and Timo Feeva et al. model [22]. These measurements showed good agreement with the Wasp model. Figures (16) and (17) reveal the thermal conductivity ratio for the two types of nanoparticles Cu and TiO_2 with three types of the base fluids DW, EG, EG + DW. As well as the measurements for Cp compared with two models of *C*p [23,24] and reveal in Figures (18) and (19). The second model showed good agreement with measurements. Figures (20) and (21) depicted specific heat for the six types of of nanofluids**.** (μ, ρ, k and C_P) are increase of about 10.25%, 5.33%, 16% and 7.2% respectively for the first type of nanoparticle while increased about 8.12%, 3.62%, 11.9% and 2.95% for the second type of nanoparticle at 5 vol% and 25^{0}C compared with that of distilled water.

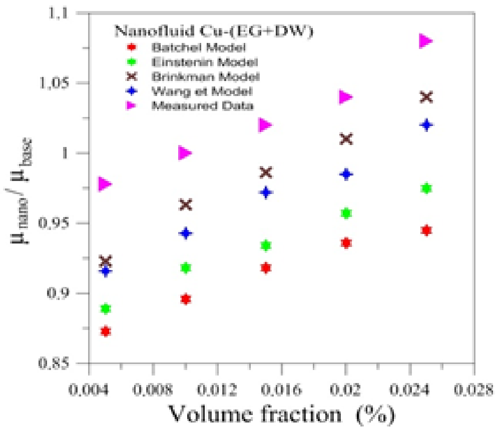

Fig. 6. Viscosity ratio for Cu - (EG+DW).

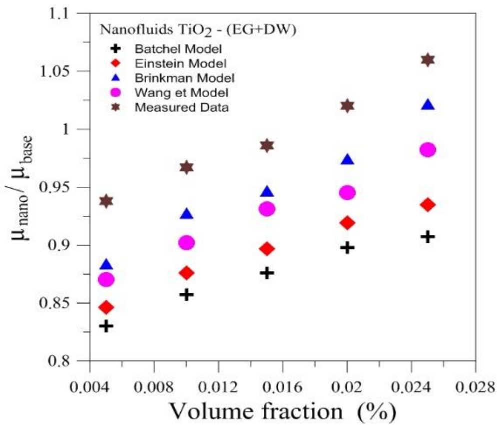

Fig. 7. Viscosity ratio for TiO_2 - (EG+DW).

Data Analysis and Validation

The heat transfer for distilled water, ethylene glycol and ethylene glycol distilled water are estimated from Eq. (1) and for nanofluid from Eq. (2). Fouling factor was not taken into account.

$$Q_W = m_W c_{Pw} (T_{in} - T_{out})_W \quad (1)$$

where: A_o surface area; q is the rate of heat transfer; and LMTD is the log mean temperature difference.

$$LMTD = \frac{(\Delta T_2 - \Delta T_1)}{\ln\left(\frac{\Delta T_2}{\Delta T_1}\right)} \quad (5)$$

Also

$$Q = h_i A_i (T_W - T_b) \quad (6)$$

$$Nu_i = \frac{h_i d_i}{k_{nf}} \quad (7)$$

where: T_W is the wall temperature, T_b is the bulk temperature, A_i is the inside area and h_i is the inner heat transfer coefficient. The U_o and h_i are calculated from Eqs. (4) and (6). The Nu_i calculated from Eq. (7). The coefficient of overall heat transfer is often

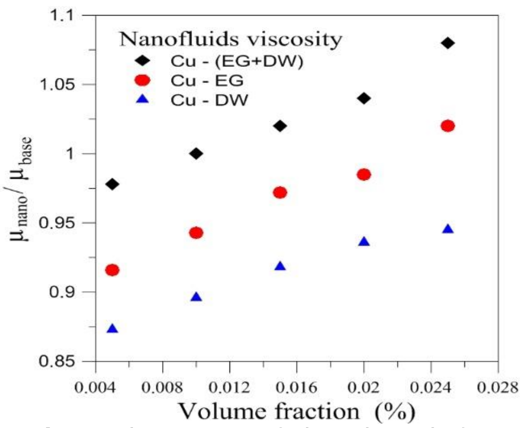

Fig. 8. Three types of viscosity ratio for Cu –DW, Cu - EG and Cu - (EG+DW).

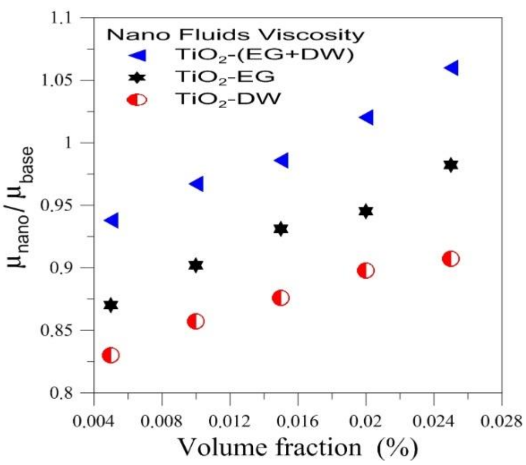

Fig. 9. Three types of viscosity ratio for TiO_2 – DW, TiO_2 – EG and TiO_2 – (EG+DW)

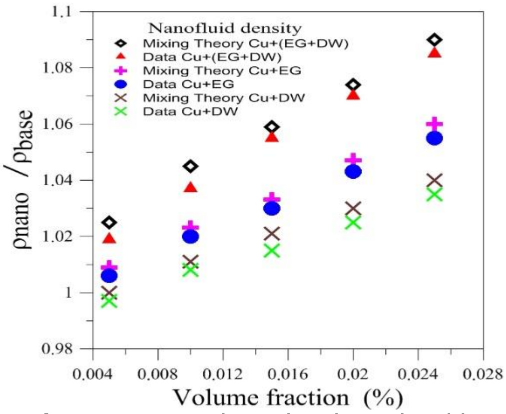

Fig. 10. Comparison density ratio with mixing theory for Cu.

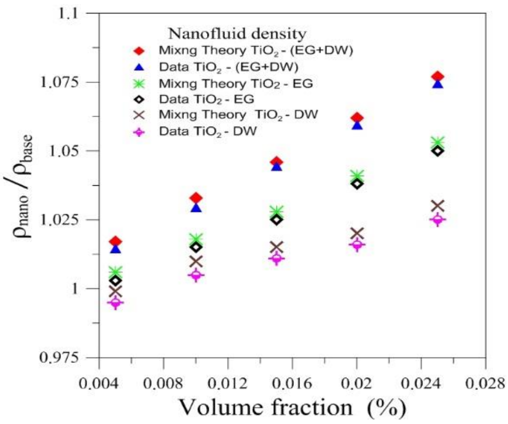

Fig. 11. Comparison density ratio with mixing theory for TiO_2.

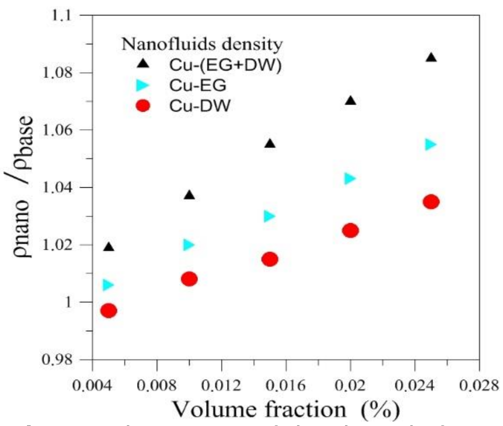

Fig. 12. Three types of density ratio for Cu.

$$Q_{nf} = m_{nf} c_{Pnf} h_{nf} (T_{in} - T_{out})_{nf} \quad (2)$$

$$q = \frac{Q_W + Q_{nf}}{2} \quad (3)$$

The temperature data and the heat transfer rate were used to calculate the overall heat transfer coefficient, U_o, as following [25]:

$$U_o = \frac{q}{A_o\, LMTD} \qquad (4)$$

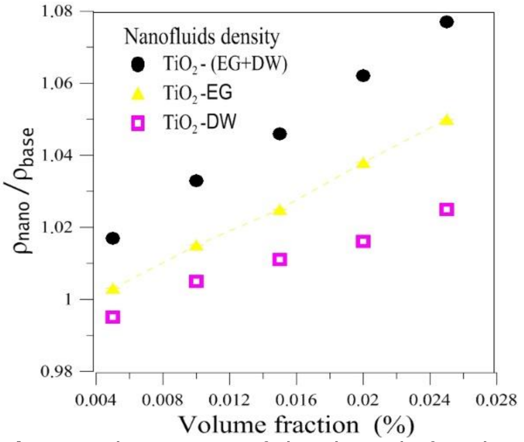

Fig. 13. Three types of density ratio for TiO_2.

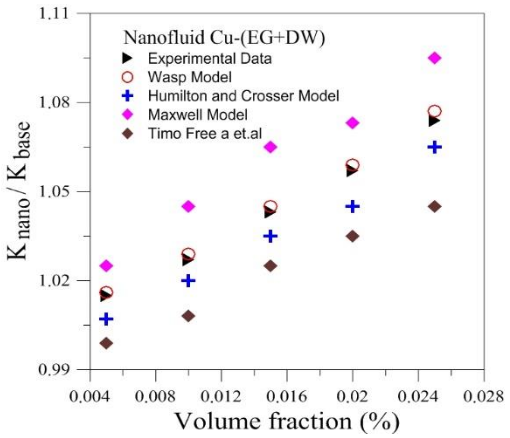

Fig. 14. Thermal conductivity ratio for Cu –(EG+DW).

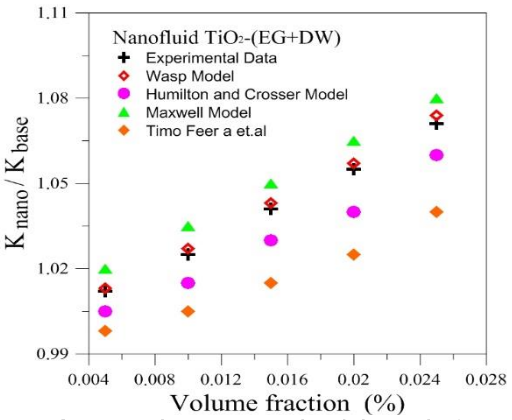

Fig. 15. Thermal conductivity ratio for TiO_2 –(EG+DW).

associated with the inner and outer heat transfer coefficients by the subsequent equation [25]:

$$\frac{1}{U_o} = \frac{A_o}{A_o\, h_i} + \frac{A_o \ln\left(\frac{D_i}{d}\right)}{2\pi k L} + \frac{1}{h_i} \qquad (8)$$

The Nusslet number in shell side of heat exchanger is calculate as following.

$$Nu_o = \frac{h_o D_h}{k_{nf}} \qquad (9)$$

where: D_h is the shell hydraulic diameter is calculate from the following:

$$D_h = \frac{4(V_{\text{shell}} - V_{\text{tube}})}{\pi(D+d)(L_{\text{shell}} + L_{\text{tube}})} \qquad (10)$$

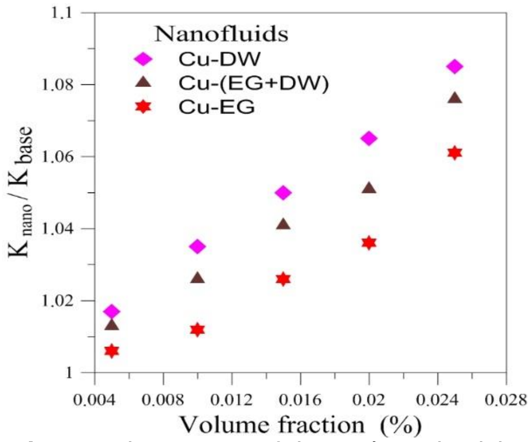

Fig. 16. Three types of thermal conductivity ratio for Cu.

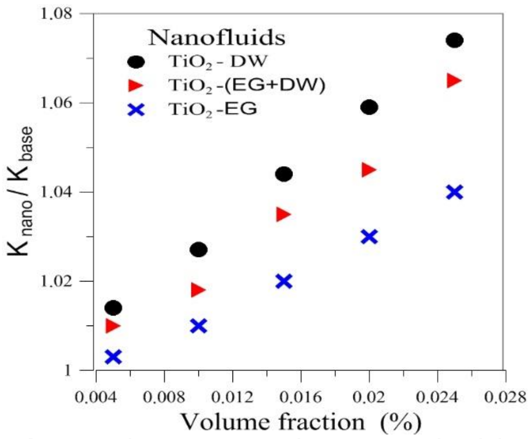

Fig. 17. Three types of thermal conductivity ratio for TiO_2.

Similarly, to the coefficient of heat transfer, the nanofluids flowing friction factor via the heat exchanger was calculate as following.

$$f_{nf} = \frac{2D\Delta P_{nf}}{L\rho_{nf} u_{nf}^2} \qquad (11)$$

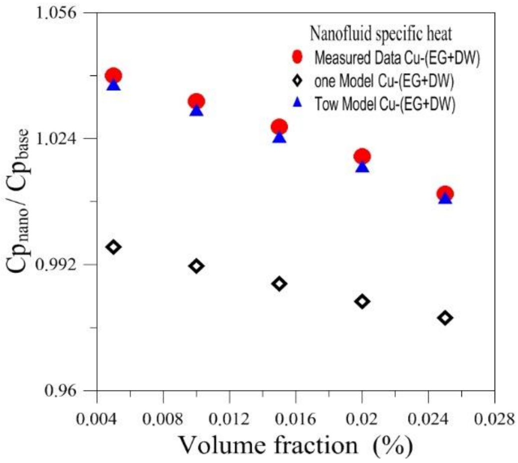

Fig. 18. Specific heat ratio for Cu – (EG+DW).

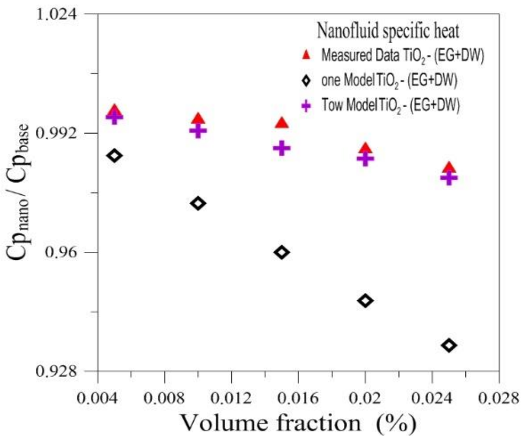

Fig. 19. Specific heat ratio for TiO_2– (EG+DW).

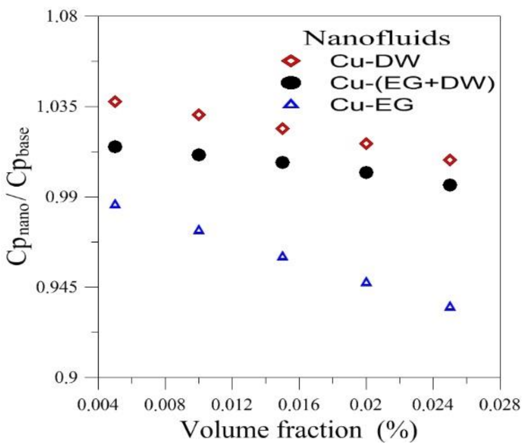

Fig. 20. Three types of specific heat ratio for Cu.

where: f_{nf} is the nanofluid friction factor, $\Delta P_{nf}$is the nanofluid measured pressure drop, L is the tube length, ρ_{nf} is the nanofluid density, and u_n is the nanofluid velocity mean. The empirical relations for the properties of nanofluids were compared with experimental measurements viscosity, density, thermal conductivity and specific heat.

A. The models for nanofluid viscosity

Equation	Ref.
$\mu_{nf} = (1+2.5\phi)\mu_{nf}$	[14]
$\mu_{nf} = (1-\phi)^{-2.5}\mu_{bf}$	[15]
$\mu_{nf} = (1+7.3\phi+123\phi^2)\mu_{bf}$	[16]
$\mu_{nf} = (1+2.5\phi+6.2\phi^2)\mu_{bf}$	[17]

A. The model for nanofluid density.

Equation	Ref.
$\rho_{nf} = (1-\phi)\rho_{bf} + \phi\rho_{bf}$	[18]

A. The models for nanofluid thermal conductivity [19–22].

$$k_{nf} = \frac{k_b + (n-1)k_b - (n-1)\left(k_b - k_p\right)\phi}{k_b - (n-1)k_b + \left(k_b - k_p\right)\phi}k$$

$$k_{nf} = \left[\frac{k_b + 2k_b + 2\left(k_b - k_p\right)\phi}{k_b + 2k_b - \left(k_b - k_p\right)\phi}\right]k_b$$

$$k_{nf} = (1+3\phi)k_p$$

B. The models for nanofluid specific heat.

Equation	Ref.
$c_{nf} = (1-\phi)c_{bf} + \phi c_P$	[23]
$c_{nf} = \frac{(1-\phi)(\rho c)_{bf}+\phi(\rho c)_P}{\rho}$	[24]

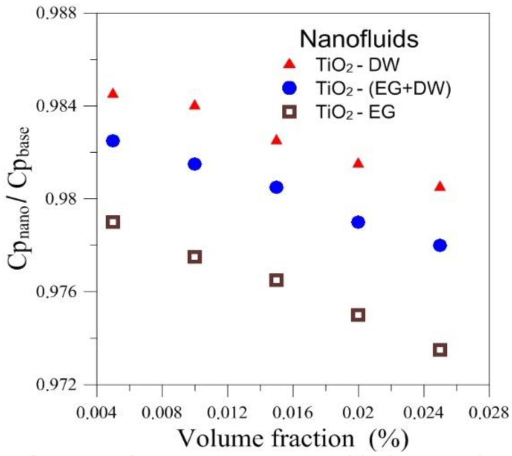

Fig. 21. Three types of specific heat ratio for TiO_2.

Results and Discussion

In this article the experimental data for the friction factors and coefficient of heat transfer are compared with data from the Shokouhm and Salimpour [26] and Salimpour [27] for flow in helical coiled heat exchanger which are defined as follows:

$$Nu_i = 0.112De^{0.51}\gamma^{-0.37}Pr^{0.72} \quad (12)$$

$$Nu_o = 5.48Re^{0.511}\gamma^{0.546}Pr^{0.226} \quad (13)$$

The friction factor for turbulent flow in helical coiled tube, f, is determined as [28].

$$f_c = \frac{7.0144}{Re}\sqrt{De} \quad (14)$$

Figures (22) and (23) show the good agreement between the practical data and calculated data when using Dw. Figures (24) to (26) reveal the Uo of counter flow versus the Uo of parallel flow and using three types nanofluids (Cu –DW,Cu – EG and CU – (EG +DW)). These figures indicated that their good agreement between data. The Uo for counter flow is (6–12)% greater than the Uo for parallel flow at 0.5 vol % and using three types of nanofluids (Cu –DW,Cu – EG and CU – (EG +DW)). The Uo for counter flow is (25–52)% greater than the Uo for parallel flow at 5 vol% and using the same three types of nanofluids. This means that insignificant impact for heat transfer flow condition changing and the reason is lead to the primary and secondary flow in tube side will be perpendicular on the flow in shell side. The flow direction changing does not impact on Uo. The results from the counter flow configuration were similar to the parallel flow. Heat transfer rates, however, are much higher in the counter flow configuration, due the increased log mean temperature difference.

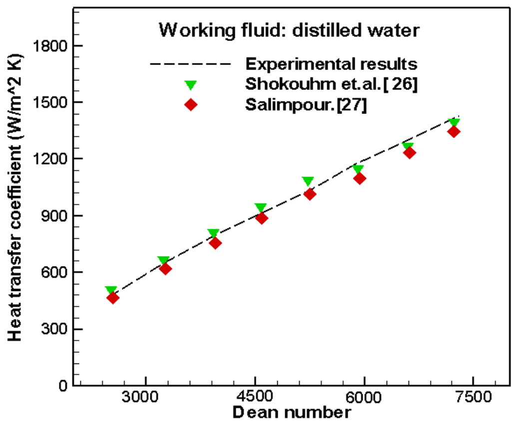

Fig. 22. Comparison between measured heat transfer coefficient and that and that calculated from [26,27].

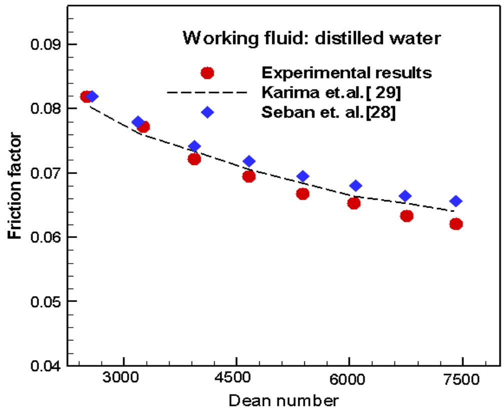

Fig. 23. Comparison between measured friction factor calculated from [28,29].

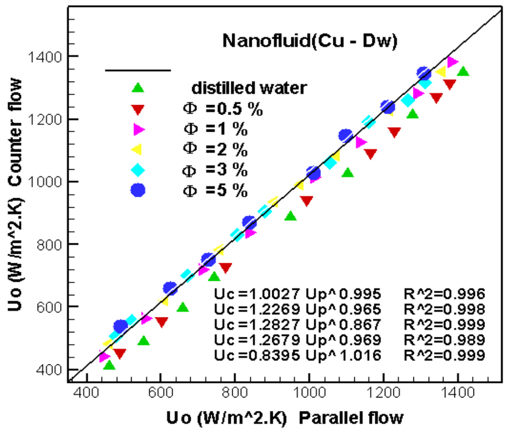

Fig. 24. Overall heat transfer coefficient for two types flow configuration (counter and parallel) to Cu – DW nanofluid.

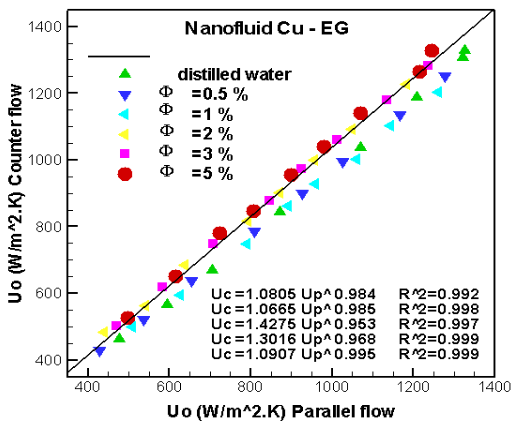

Fig. 25. Overall heat transfer coefficient for two types flow configuration (counter and parallel) to Cu – EG nanofluid.

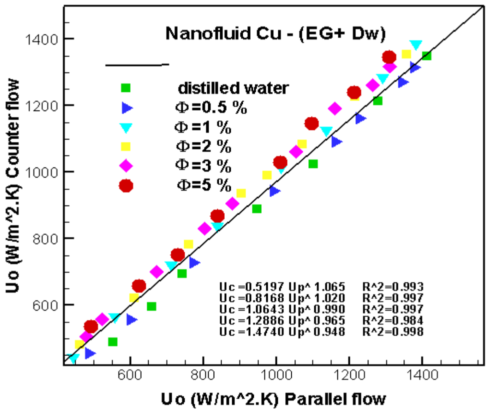

Fig. 26. Overall heat transfer coefficient for two types flow configuration (counter and parallel) to Cu – (EG+DW) nanofluid.

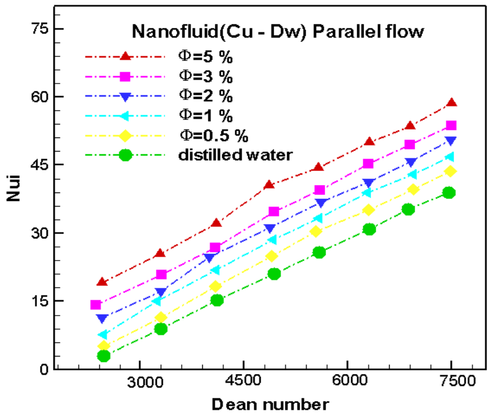

Fig. 27. Variation of Nui to nanofluid (Cu-DW) and counter flow.

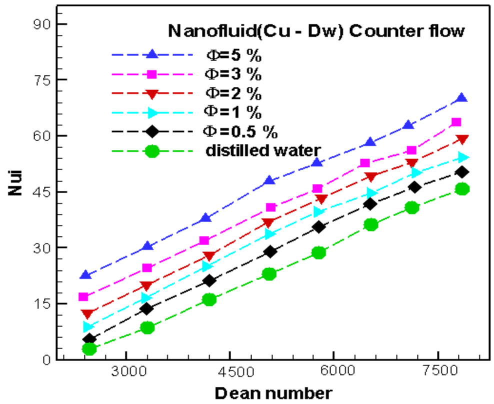

Fig. 28. Variation of Nui to nanofluid (Cu-DW) and parallel flow.

Figures (27) to (38) reveal the changing of Nu_i with De for both parallel and counter flow. These figures indicated that insignificant impact on the Nui when using nanofluids (Cu –DW,Cu – EG,CU – (EG +DW), TiO_2 –DW, TiO_2 – EG and TiO_2 – (EG +DW)). this reason the flow configuration and the hi is the same. Also the centrifugal force and the secondary flow did not obtain negative effect. The Nu_i increases with ϕ.

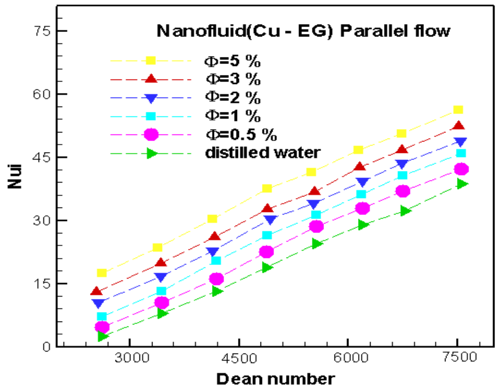

Fig. 29. Variation of Nu_i to nanofluid (Cu–EG) and parallel flow.

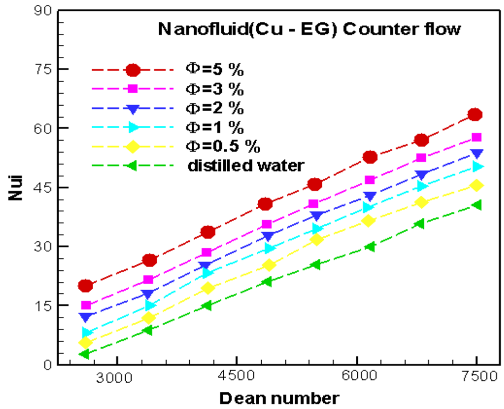

Fig. 30. Variation of Nu_i to nanofluid (Cu–EG) and counter flow.

In general the thermal conductivity is proportional with the convective heat transfer. The experimentally determined coefficients of friction of nanofluids are shown in Figs. (39) to (44). The experimental coefficient of friction results of TiO_2 at 0.5%, 1%, 2%, 3% and 5% particle volume concentration is shown in these figures, solid line indicates the experimentally results of distilled water and the symbols indicate the nanofluids for turbulent flow. The friction factor of nanofluids (TiO_2 –DW, TiO_2–EG and TiO_2–(EG+DW)) proportional with the friction factor of distilled water at low volume fraction concentration for spiral coil heat exchanger. These figures shown the coefficient of friction of TiO_2 is slightly increased compared with that of distilled water at high volume fraction concentration due to nanoparticles suspension in Dw. Most TiO_2 data was located above the line distilled water. The friction factor in the spiral coil heat exchanger was insignificant impact with changing concentrations of nanopar-ticles.

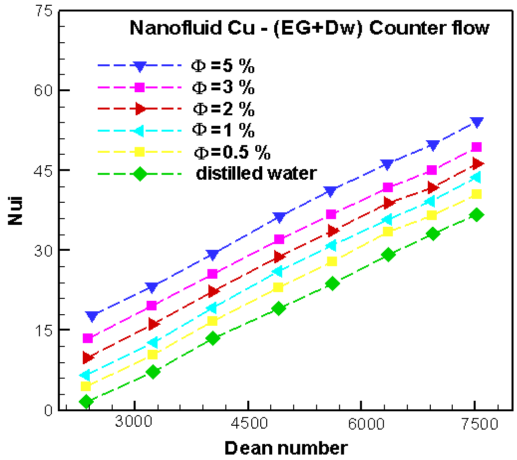

Fig. 32. Variation of Nu_i to nanofluid Cu – (EG + Dw) and counter flow.

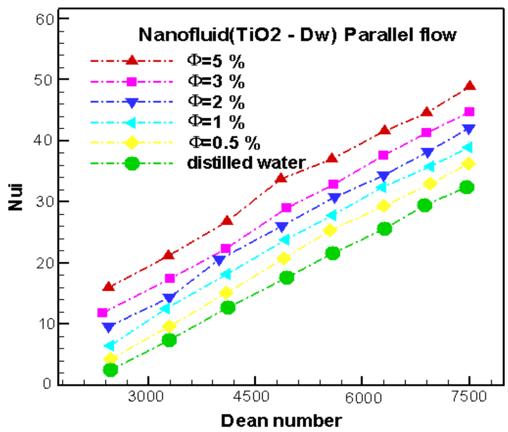

Fig. 33. Variation of Nu_i to nanofluid (TiO_2 –DW) and parallel flow.

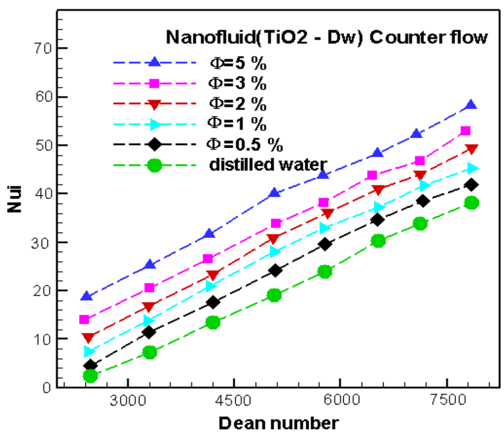

Fig. 34. Variation of Nu_i to nanofluid (TiO_2 –DW) and counter flow.

In this case not need pumping power and a penalty in pressure drop when using nanofluid due to small nanoparticles suspension in Dw which not the change of the behavior of nanofluid flow. The pressure drop to base fluid of ethylene glycol is smaller than the base fluid of distilled water.

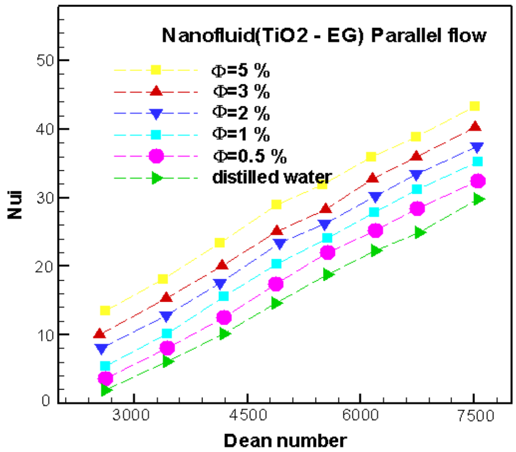

Fig. 35. Variation of Nu_i to nanofluid (TiO_2 –EG) and parallel flow.

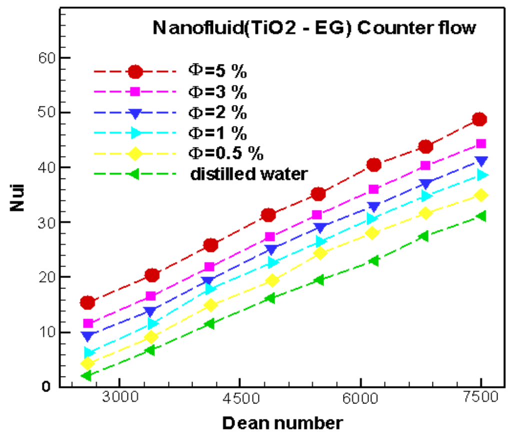

Fig. 36. Variation of Nu_i to nanofluid (TiO_2 –EG) and counter flow.

Figures (45) to (50) show shear stress versus shear rate for nanofluids (Cu–DW,Cu–EG and CU–(EG+DW) at 0.5%, 1%, 2%, 3% and 5% particle volume concentra-tion. These figures indicating that the nanop-articles and distilled water are Newtonian fluid. As well as these figures indicated the shear stress increases with an increasing shear rate, for nanofluids Cu–DW, Cu–EG and CU–(EG+DW).

These figures indicated the flow curve of the nanofluids measured using a spiral coil heat exchanger. The shear stress increases with volume fraction for parallel and counter flow nanofluids. The use of nanofluid significant gives higher Nusselt number than distilled water and ethylene glycol as based fluids. Also the results indicated that an increase in *h* of 50.2% to Cu–Dw, 41.5% to Cu–(EG+Dw), 32.12% to Cu–EG and 36.5%. to TiO_2 – DW, 30.2 % for TiO_2 – (EG + DW), 25.5%, for TiO_2 – EG .

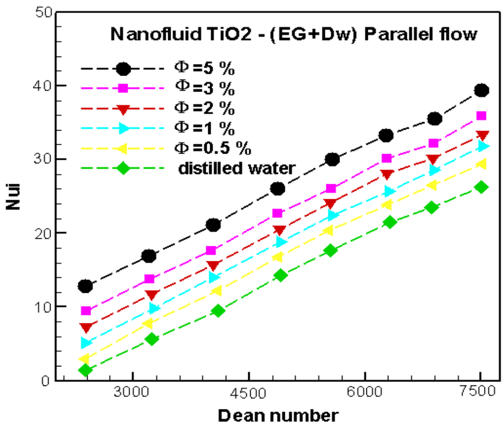

Fig. 37. Variation of Nu_i to nanofluid TiO_2 – (EG + DW) and parallel flow.

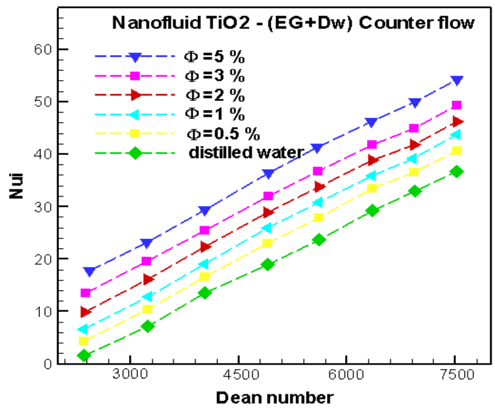

Fig. 38. Variation of Nu_i to nanofluid TiO_2 – (EG + Dw) and counter flow.

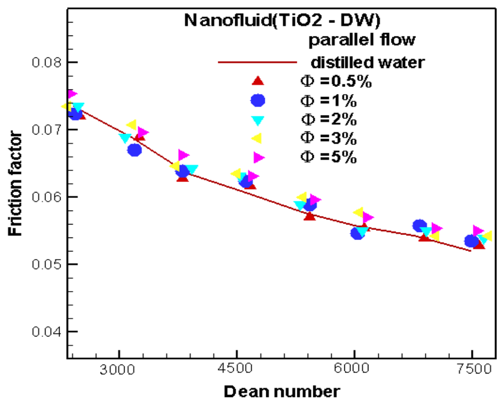

Fig. 39. The friction factor for nanofluid (TiO_2 –DW) and parallel flow.

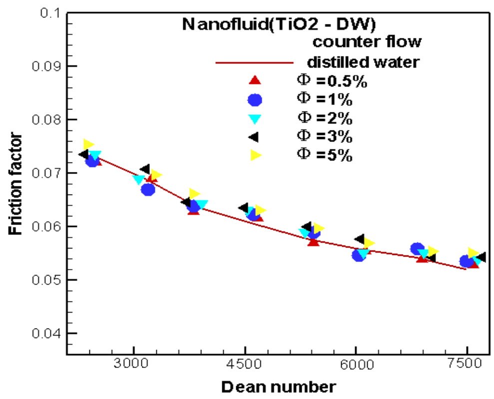

Fig. 40. The friction factor for nanofluid (TiO_2 – DW) and counter flow.

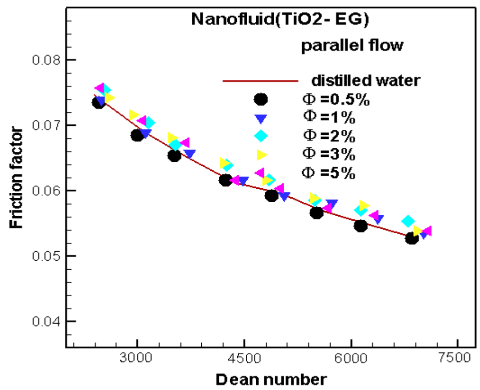

Fig. 41. The friction factor for nanofluid (TiO_2 – EG) and parallel flow.

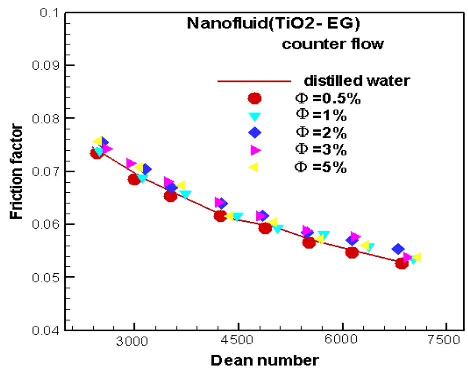

Fig. 42. The friction factor for nanofluid (TiO_2 – EG) and counter flow.

The presence of nanoparticles (Cu and TiO_2) is produces strong nano convection current and good mixing. The enhancements in metal nanofluids are better than the oxide metal nanofluids. The coefficient of overall heat transfer is insignificant impact on flow direction change and the nanofluids behaves as the Newtonian fluid for 0.5%, 1%, 2%, 3% and 5%. The practical data for fricaton coefficient of nanofluid show that their good

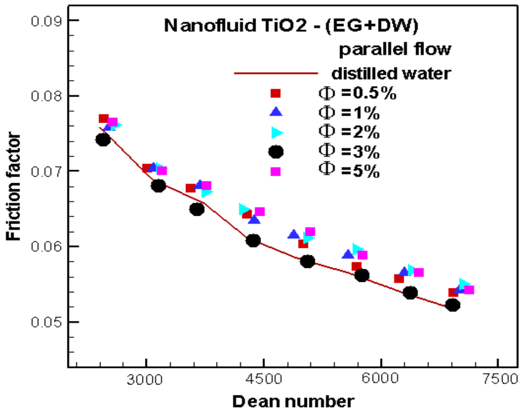

Fig. 43. The friction factor for nanofluid TiO_2 – (EG +DW) and parallel flow.

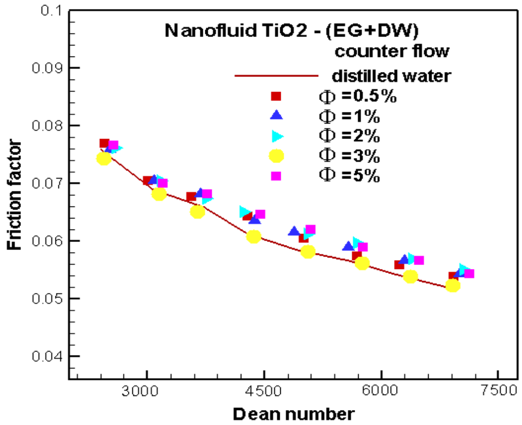

Fig. 44. The friction factor for nanofluid TiO_2 – (EG +DW) and counter flow.

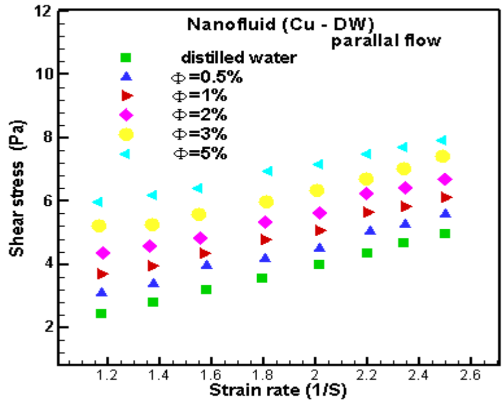

Fig. 45. Shear stress against shear rate for nanofluid (Cu–DW) and parallel flow.

agreement with data of the Colebrook formula. This means that not need pumping power and a penalty in pressure drop when using nanofluid which make appropriate in experimental applications. This study reveal that the thermal performance from nanofluid Cu–DW is higher than Cu–(EG+DW) and Cu–EG due to higher thermal conductivity for the silver and distilled water compared with ethylene glycol.

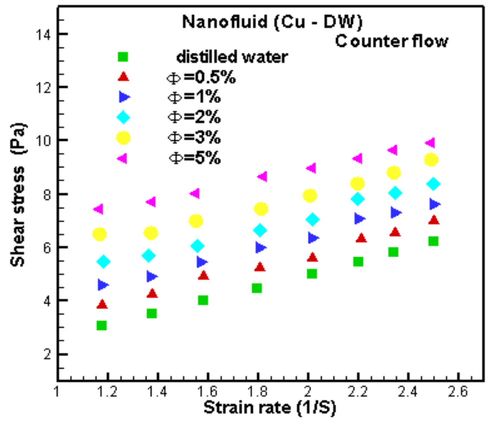

Fig. 46. Shear stress against shear rate for nanofluid (Cu – DW) and counter flow.

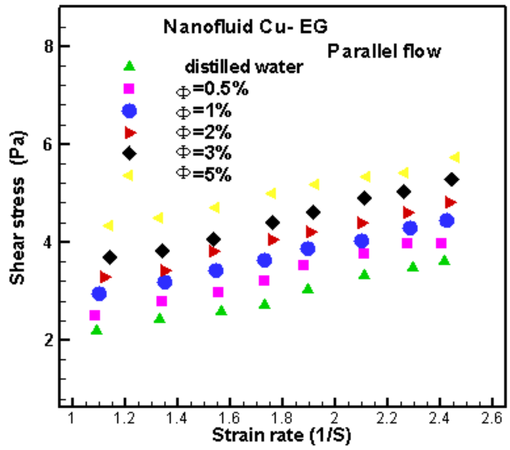

Fig. 47. Shear stress against shear rate for nanofluid (Cu –EG) and parallel flow.

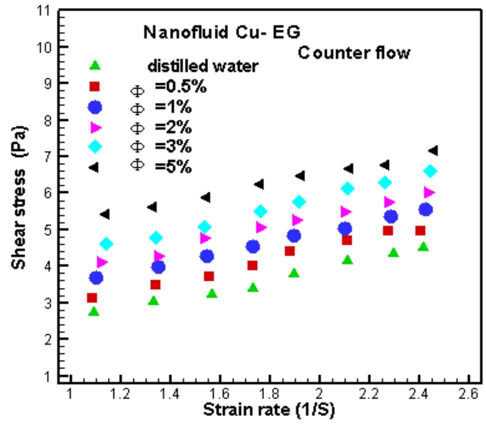

Fig. 48. Shear stress against shear rate for nanofluid (Cu –EG) and counter flow.

Conclusions

The main conclusions of the present experimental article were as follows:

1. The type of nanoparticles and base fluid was play role important in improvement of heat transfer by using nanofluids.
2. The presence of Cu and TiO_2 nanoparticles attributes to the generation is obtained better mixing.
3. The coefficient of overall heat transfer was insignificant impact on changing of flow direction of nanofluid (Cu–DW,Cu –EG and CU – (EG +DW), TiO_2 –DW, TiO_2 – EG and TiO_2 – (EG +DW)) behaves as a Newtonian fluid for 0.5%,1%, 2%, 3% and 5%.
4. The improvement of metal nanofluid was better than the oxide metal of nanofluids.

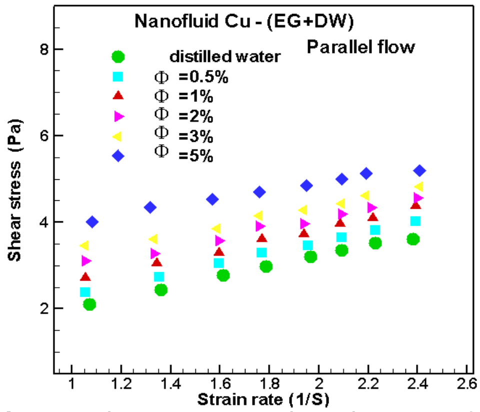

Fig. 49. Shear stress against shear rate for nanofluid Cu – (EG+DW) and counter flow.

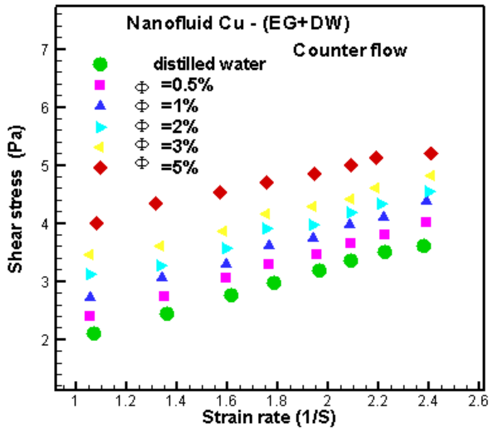

Fig. 50. Shear stress against shear rate for nanofluid Cu–(EG+DW) and parallel flow.

5. The improvement of nanofluid not only increases of the thermal conductivity But there are other parameters i.e., viscosity of nanofluid, base fluid.
6. The shear stress of nanofluids increases with volume fraction of the nanoparticles to parallel and counter flow.
7. The nanofluid with Dw is the same nearly for the pressure drop and friction coefficient while nanofluid with ethylene glycol is smaller than EG. This means that no need for pumping power and a penalty in pressure drop.

References

[1] Pak B, Cho Y. Hydrodynamic and heat transfer study of dispersed fluids with submicron metallic oxide particles. Experimental Heat Transfer 1998;**11**: 151-170.

[2] Lee S, Choi S, Li S, Eastman JA. Measuring thermal conductivity of fluids containing oxide nanoparticles. ASME Journal Heat Transfer 1999;**121**:280–289.

[3] Wang X, Xu X, Choi S. Thermal conductivity of nanoparticle – fluid mixt-ure. Journal of Thermophysics and Heat Transfer 1999;**13**:474–480.

[4] Xuan Y, Li Q. Heat transfer enhancement of nanofluids. Internatio-nal Journal of Heat and Fluid Flow 2000;**21**:58–64.

[5] Xuan Y, Roetzel W. Conceptions for heat transfer correlation of nanofluids. International Journal of Heat and Mass Transfer 2000;**43**:3701–3707.

[6] Das SK, Putra N, Thiesen P, Roetzel W. Temperature dependence of thermal conductivity enhancement for nanofl-uids. ASME Journal of Heat Transfer 2003;**125**:567–574.

[7] Yang Y, Zhang ZG, Grukle AK, Anderson WB, Wu G. Heat transfer properties of nanoparticle-in-fluid disper-sions (nanofluids) in laminar flow. International Journal of Heat and Mass Transfer 2005;**48**:1107–1116.

[8] Koo J, Kleinstreuer C. Impact analysis of nanoparticle motion mechanisms on the thermal conductivity of nanofluids. Inter-national Communications in Heat and Mass Transfer 2005;**32**:1111–1118.

[9] Heris SZ, Esfahany MN, Etemad SGh. Experimental investigation of convective heat transfer of Al_2O_3 / water nanofluid in circular tube. International Journal of Heat and Fluid Flow 2007;**28**:203–210.

[10] Zhang X, Gu H, Fujii M. Effective thermal conductivity and thermal diffusivity of nanofluids containing spherical and cyli-ndrical nanoparticles. Experimental Thermal and Fluid Sciences 2007;**31**: 593–599.

[11] Seban RA, McLaughlin EF. Heat transfer in tube coils with laminar and turbulent flow. International Journal of

Heat and Mass Transfer 1963;**6**:387–395.
[12] Regers GFC, Mayhew YR. Heat transfer and pressure loss in helically coiled tubes with turbulent flow. International Journal of Heat and Mass Transfer 1964;**7**:1207–1216.
[13] Mori Y, Nakayama W. Study on forced convective heat transfer in curved pipe. International Journal of heat and Mass Transfer 1965;**8**:67–82.
[14] Einstein A. Investigation on the theory of Brownian motion. Dover; New York: 1956.
[15] Binkman HC. The viscosity of concentrated suspensions and solution. The Journal of Chemical Physics 1952;**20**(4):571.
[16] Wang X, Xu X, Choi S. Thermal conductivity of nanoparticle – fluid mixture. Journal of Thermophysics and Heat Transfer 1999;**13**:474–480.
[17] Batchelor GK. The effect of Brownian motion on the bulk stress in a suspension of spherical particles. Journal of Fluid Mechanics 1977;**83**(1): 97-117.
[18] Smith JM, Van Ness HC. Introduction to chemical engineering thermodynamic. McGraw-Hill: New York; 1987.
[19] Wasp EJ, Kenny JP, Gandhi RL. Solid – liquid slurry pipeline transportation, bulk materials handling. Transtechnology Publications: Germany;1999.
[20] Hamilton RL, Crosser OK. Thermal conductivity of heterogeneous two-component systems. Industrial & Engineering Chemistry Fundamentals 1962;**1**(3): 187-191.
[21] Maxwell JC. A treatise on electricity and magnetism. Second ed. Clarendon Press Oxford: UK;1981.
[22] Timofeeva EV, et al. Thermal conductivity and particle agglomeration in alumina nanofluids. Experiment and Theory. Physical Review E Journal 2007;**76**(6): 16-23.
[23] Xuan Y, Roetzel W. Conceptions for heat transfer correlation of nanofluids. International Journal of Heat and Mass Transfer 2000;**43**:3701–3707.
[24] Pak BC, Cho YI. Hydrodynamic and heat transfer study of dispersed fluids with sub micro metallic oxide particles. Experimental Heat Transfer 1998;**11**: 151-170.
[25] White FM. Heat transfer. Addison–Wesley Publishing Company Inc.: New York;1984.
[26] Shokouhm H, Salimpour MR, Akhavan MA. Experimental investigation of shell and coiled tube heat exchangers using Wilson plots, International Communications in Heat and Mass Transfer 2008;**35**: 84–92.
[27] Salimpour MR. Heat transfer characteristics of a temperature–dependent property fluid in shell and coiled tube heat exchangers. International Communications in Heat and Mass Transfer 2008;**35**:1190–1195.
[28] Seban RA, Mclauchlin EF. Heat transfer in tube coils with laminar and turbulent flow. Heat Mass Transfer 1962;**6**:387–395.
[29] Amori KE, Sherza JS. An investigation of shell–helical coiled tube heat exchanger used for solar water heating system. Innovative Systems Design and Engineering 2013;**4**(15):78-90.